Electronic Supplementary Material (ESI) for Dalton Transactions.

Supporting Information

Redox Active Ligand and Metal Cooperation for C(sp^2)-H Oxidation: Extension of Galactose Oxidase Mechanism in Water-Mediated Amide Formation

Zahra Alaji,[a] Elham Safaei*,[a, b] Hong Yi,[c] Hengjiang Cong,[c] Andrzej Wojtczak,[d] Aiwen Lei*,[c]

[a]Institute for Advanced Studies in Basic Sciences (IASBS), 45137-66731, Zanjan, Iran.

[b]Department of Chemistry, College of Sciences, Shiraz University, 71454, Shiraz, Iran.
Email: e.safaei@shirazu.ac.ir

[c]College of Chemistry and Molecular Sciences, Institute for Advanced Studies (IAS), Wuhan University, Wuhan, Hubei 430072, P. R. China.
Email: aiwenlei@whu.edu.cn

[d]Nicolaus Copernicus University, Faculty of Chemistry, 87-100 Torun, Poland

Content

Materials and Physical Methods

All reagents and solvents were purchased from commercial sources and were used as received, unless noted otherwise. Anhydrous $Cu(OAc)_2$, 98%. Super dry acetonitrile, dichloromethane were used for synthesis and growing crystal as mentioned. Preparation and handling of air- and moisture-sensitive materials were carried out under an inert gas atmosphere of glove box.
NMR spectra were recorded at 400 MHz on a Bruker DRX spectrometer in $CDCl_3$ solution. The chemical shifts were referred to TMS using the residual signals from the solvent.
IR spectra were recorded in the solid state on a FT-IR Bruker Vector 22 spectrophotometer in the 400−4000 cm^{-1} range.
LC-MS mass spectral data were acquired on Shimadzu LCMS 2020.
HRMS spectra were recorded on thermo Fisher scientific LTQ Orbitrap Elite.
Cyclic Voltammetry (CV) was performed on CHI605E, CH Instruments, USA, equipped with a Ag wire reference electrode, a glassy carbon working electrode, and a Pt counter electrode with 0.1 M $Bu_4N(BF_4)$ solutions in CH_2Cl_2. Ferrocene was used as an internal standard.

X-ray Crystallographic Analyses

All crystals were placed onto the tip of a 0.1 mm diameter glass capillary and mounted on a Bruker SMART Platform CCD diffractometer for data collection. The data collections were carried out using MoKαradiation with a graphite monochromator (λ= 0.71073 A) at 95 K. Structure solutions were performed by direct methods using SHELXS-97 software and refined against F2using full-matrix-least-squares using SHELXL-97 and SHELXL-2013 software. Data intensities were corrected for absorption and decay (SADABS). Final cell constants were obtained from least squares fits of all measured reflections. All non-hydrogen atoms were refined with anisotropic displacement parameters.

Material Synthesis

To a solution of 3,5-DTBQ (3,5-di-tert-butylcyclohexa-3,5-diene-1,2-dione) (0.22 g, 1 mmol) in acetonitrile (4 mL) was added 2-aminobenzyl amine (0.122 g, 1 mmol), and the reaction solution stirred for 30 min at the room temperature in the presence of air. After some minutes, it afforded a yellow precipitate (scheme S1).
^{1}H NMR (400 MHz, Chloroform-*d*) δ 8.70 (s, 1H), 7.46 (dd, 1H), 7.28 (dt, 2H), 7.05 (d, 1H), 6.79 (m, 2H), 6.71 (s, 1H), 6.27 (s, 2H), 1.51 (s, 9H), 1.40 (s, 9H)

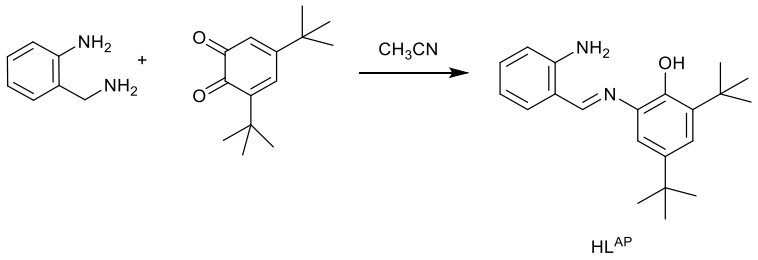

Scheme S1. Synthesis of HL^{AP} ligand

Next, to the stirred suspension of HL^{AP} (0.324 g, 1 mmol) in acetonitrile was added pyridine-2-carboxaldehyde (0.096 mL, 1 mmol) (Scheme S2). LC-MS data clearly shows the formation of this ligand (Figure S1).
This ligand (HL^{IPIP}) is stable at dry and inert condition. When it is exposed on moisture, it is hydrolyzed. Therefore, after one minute stirring, different metal precursors of copper, zinc and nickel were added to reaction mixture to afford the metal complexes (Scheme S3).

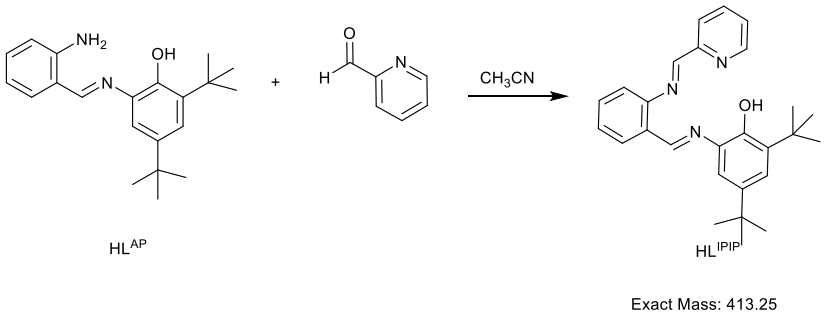

Scheme S2. Synthesis of HL^{IPIP} ligand

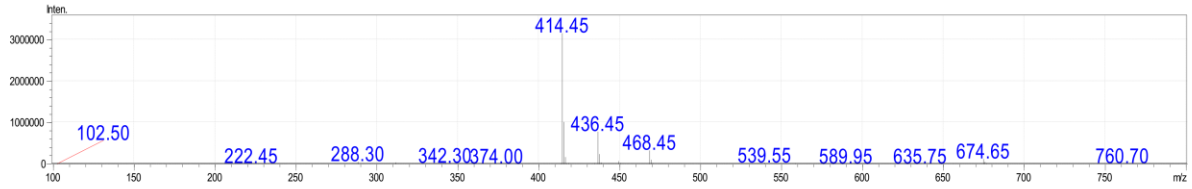

Figure S1. LC-MS spectrum of HL^{IPIP}

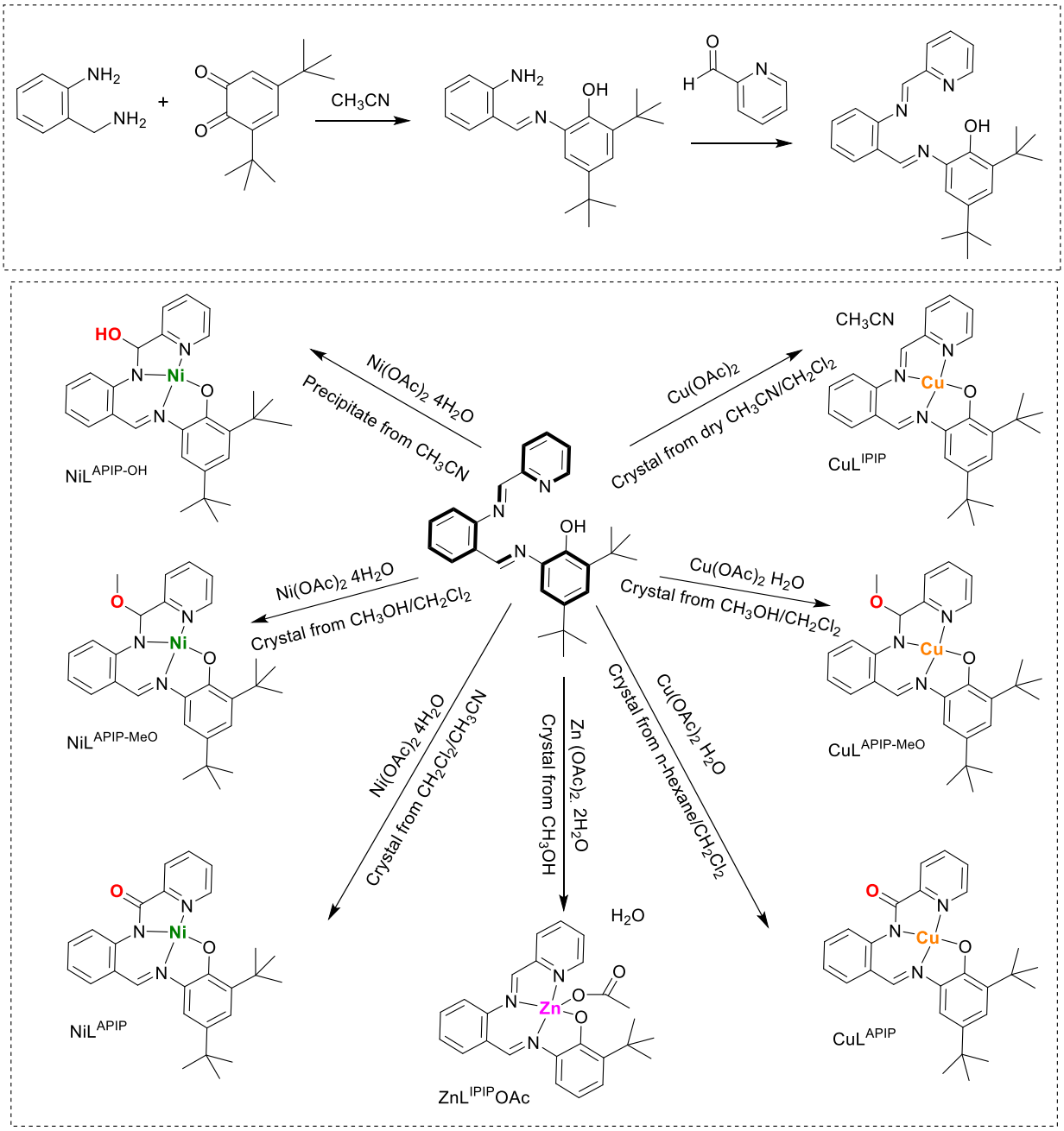

Scheme 3. General scheme for the preparation of the different metal complexes

Synthesis of $Cu^{II}L^{APIP}$

$Cu^{II}L^{APIP}$ complex was synthesized by the following template reaction. Firstly, to the stirred suspension of HL^{AP} (0.324 g, 1 mmol) in acetonitrile was added pyridine-2-carboxaldehyde (0.096 mL, 1 mmol), after one minute stirring $Cu(OAc)_2{\cdot}H_2O$ (0.199 g, 1 mmol) was added in the presence of 2 equivalents of NEt_3 to the reaction mixture.

The stirring of red-brown solution at 298 K for 4 h afforded a red-brown precipitate of copper complex. The filtrate was left undisturbed to afford red brown microcrystals (0.309 g, 63% yield) by evaporation from dichloromethane/acetonitrile solution. X-ray quality dark red single crystals were grown from a 1:1 solvent mixture of n-hexane/dichloromethane. Elemental Analysis: calculated (found) for $C_{27}H_{29}N_3O_2Cu{\cdot}0.35\ C_6H_{14}$: C 67.05, H 6.55, N 8.06; Found: C 66.79, H 6.61, N 7.76. ν_{max}(KBr)/cm^{-1}: 2959 (C-H), 1642(C=O), 1466 (C=N), 802 (=C-H bending). ESI-MS m/z : 491.2.

Synthesis of $Cu^{II}L^{IPIP}$

$Cu^{II}L^{IPIP}$ complex was synthesized by the following template reaction. Firstly, to a stirred suspension of HL^{AP} (0.324 g, 1 mmol) in dry acetonitrile was added pyridine-2-carboxaldehyde (0.096 mL, 1 mmol). Next, $Cu(OAc)_2$ (0.181 g, 1 mmol) was added to the reaction mixture. The stirring of orange-brown solution at 298 K for 4 h afforded a dark orange precipitate of copper complex.
X-ray quality dark red single crystals from were grown from dry acetonitrile/dichloromethane. ESI-MS m/z (%):476.1751

Synthesis of $Cu^{II}L^{APIP\text{-}Meo}$

To a stirred suspension of HL^{AP} (0.324 g, 1 mmol) in acetonitrile was added pyridine-2-carboxaldehyde (0.096 mL, 1 mmol). After one minute stirring, Cu $(OAc)_2{\cdot}H_2O$ (0.199 g, 1 mmol) was added in the presence of 2 equivalents of NEt_3 to the reaction mixture. The stirring of red-brown solution at 298 K for 4 h afforded a red-brown precipitate X-ray quality dark red single crystals were grown from a 1:1 solvent mixture of methanol/dichloromethane.

Synthesis of $ZnL^{IPIP}OAc$

As reported, to a stirred suspension of HL^{AP} (0.324 g, 1 mmol) in acetonitrile was added pyridine-2-carboxaldehyde (0.096 mL, 1 mmol). After one minute stirring, it was reacted immediately with Zn $(OAc)_2$. $2H_2O$ (0.219 g, 1 mmol) to afford the zinc complex of $Zn^{II}L^{IPIP}OAc$ at the ambient temperature. The stirring of black solution at 298 K for 4 h afforded a dark red-brown precipitate. X-ray quality dark crystals were grown from methanol.

ν_{max}(KBr)/cm^{-1}: 3415 (O–H), 2946 (C–H), 1606 (C=O), 1593 (C=C), 1469 (C=N), 740 (=C–H bending).

^{1}H NMR (400 MHz, $(CD_3)_2SO$): δ 1.29 (s, 9H), 1.45 (s, 9H), 1.59 (s, 3H), 7.1 (d, 1H), 7.4 (d, 1H), 7.6 (m, 2H), 7.8 (dd, 1H), 8.0 (m, 1H), 8.2 (d, 1H), 8.4 (dt, 9Hz 1H), 8.9 (m,1H), 9.0(s, 1H), 9.1(s, 1H).

^{13}C NMR (100 MHz, $(CD_3)_2SO$): δ 29.82, 30.00, 32.13, 32.21, 34.42, 35.53, 109.79, 121.03, 124.55, 128.99, 129.22, 129.63, 129.74, 132.00, 132.37, 133.54, 135.51,138.53,141.90, 145.06,147.44,149.99,153.08,161.17,162.71.

Synthesis of $Ni^{II}L^{APIP\text{-}OH}$

To a stirred suspension of HL^{AP} (0.324 g, 1 mmol) in acetonitrile was added pyridine-2-carboxaldehyde (0.096 mL, 1 mmol) under N_2 atmosphere (Figure S1). After one minute stirring, it was reacted immediately with $Ni(OAc)_2{\cdot}4H_2O$ (1 mmol, 0.248 g) to afford the nickel complex of $Ni^{II}L^{APIP}$ at the ambient temperature. The stirring of dark orange solution at 298 K for 2 h afforded a precipitate. ESI-MS m/z (%):488.1843

^{1}H NMR (400 MHz, DMSO-d_6) δ 8.80 (s, 1H), 8.60 (dt, *J* = 5.31, 1.46 Hz, 1H), 8.10 (td, *J* = 7.69, 1.57 Hz, 1H), 7.77 (dd, *J* = 7.41, 1.84 Hz, 2H), 7.64 (dd, *J* = 7.61, 5.22 Hz, 2H), 7.37 (d, *J* = 8.91 Hz, 1H), 7.24 (ddd, *J* = 8.73, 6.63, 1.74 Hz, 1H), 6.96 (d, *J* = 2.09 Hz, 1H), 6.60 (ddd, *J* = 7.75, 6.60, 0.97 Hz, 1H), 6.34 (d, *J* = 10.12 Hz, 1H), 6.07 (d, *J* = 10.06 Hz, 1H), 1.45 (s, 9H), 1.33 (s, 9H).

^{13}C NMR (101 MHz, DMSO) δ 29.76, 32.42, 34.60, 34.87, 88.40, 110.02, 113.87, 116.86, 120.66, 120.92, 124.91, 131.49, 134.54, 140.14, 141.14, 146.24, 148.21, 149.08, 160.14, 166.57.

Synthesis of $Ni^{II}L^{APIP}$

Solvent slow evaporation of $NiL^{APIP\text{-}OH}$ solution from dichloromethane/acetonitrile afforded single crystal of **$Ni^{II}L^{APIP}$**. ESI-MS m/z (%):486.1880

Synthesis of $Ni^{II}L^{IPIP}$

To a stirred suspension of HL^{AP} (0.324 g, 1 mmol) in superdry acetonitrile was added pyridine-2-carboxaldehyde (0.096 mL, 1 mmol) under N_2 atmosphere . After one minute stirring, it was reacted immediately with $Ni(OAc)_2$ (1 mmol, 0.176 g) to afford the nickel complex of $Ni^{II}L^{IPIP}$ at the ambient temperature. The stirring of dark orange solution at 298 K for 2 h afforded a precipitate. ESI-MS m/z (%):471.1808

Synthesis of $Ni^{II}L^{APIP\text{-}MeO}$

To a stirred suspension of HL^{AP} (0.324 g, 1 mmol) in acetonitrile was added pyridine-2-carboxaldehyde (0.096 mL, 1 mmol). After one minute stirring, it was reacted immediately with $Ni(OAc)_2{\cdot}4H_2O$ (1 mmol, 0.248 g) to afford the nickel complex at the ambient temperature. The stirring of dark orange solution at 298 K for 4 h afforded a precipitate. X-ray quality dark crystals were grown from dichloromethane/methanol.

^{1}H NMR (400 MHz, DMSO-d_6) δ 8.85 (s, 1H), 8.64 (ddd, *J* = 5.60, 1.54, 0.74 Hz, 1H), 8.17 (td, *J* = 7.67, 1.56 Hz, 1H), 7.87 – 7.77 (m, 2H), 7.77 – 7.65 (m, 2H), 7.38 (d, *J* = 8.84 Hz, 1H), 7.28 (ddd, *J* = 8.73, 6.66, 1.76 Hz, 1H), 6.98 (d, *J* = 2.06 Hz, 1H), 6.67 (ddd, *J* = 7.86, 6.70, 1.01 Hz, 1H), 6.30 (s, 1H), 3.01 (s, 3H), 1.45 (s, 9H), 1.33 (s, 9H).

Figures and Tables

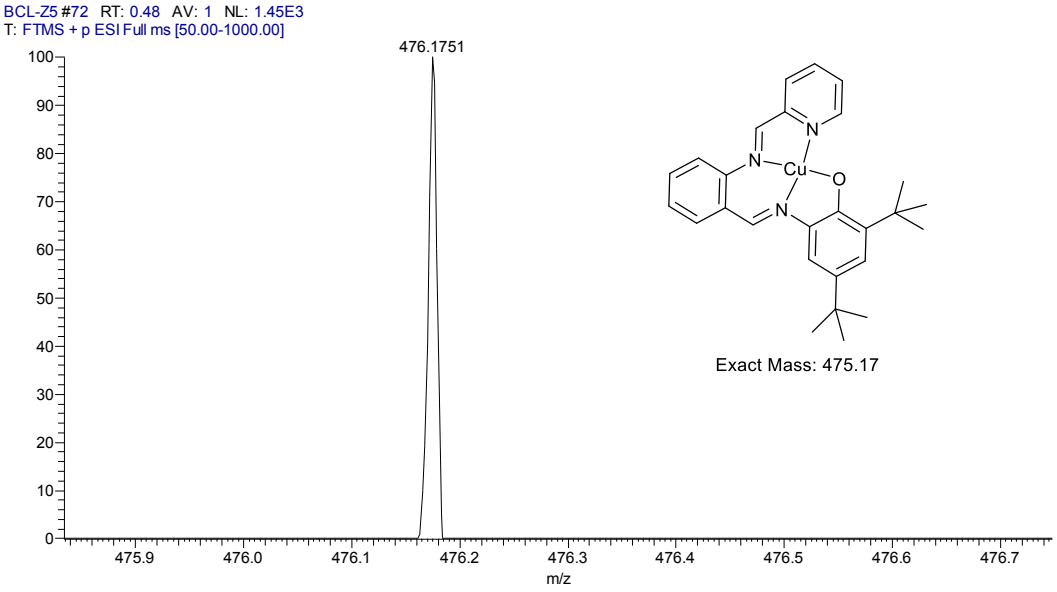

Figure S2. ESI-MS (HRMS) spectrum of CuL^{IPIP}

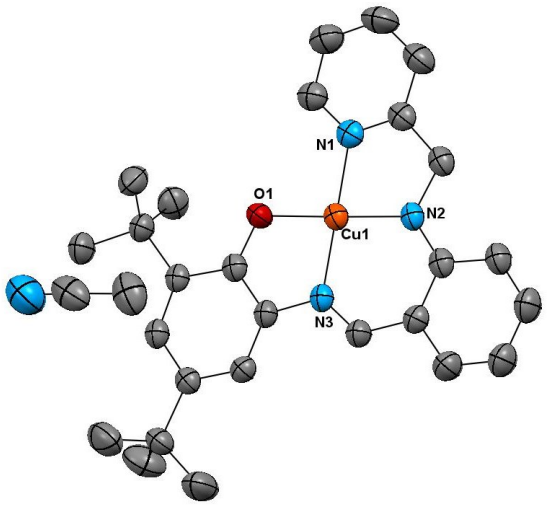

Figure S3. Molecular structure of $Cu^{II}L^{IPIP}$ ·Hydrogen atoms have been omitted for clarity. Thermal ellipsoids are set at 50 % probability. Acetonitrile molecule with the occupancy set to 50% was also found in the structure

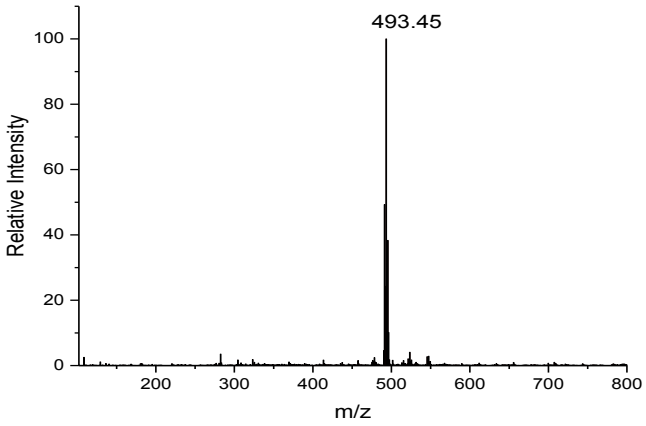

Figure S4. Isotope experiment of the reactions aminophenol-iminopyridine ligand and $Cu(OAc)_2$ in the presence of $H_2{}^{18}O$.

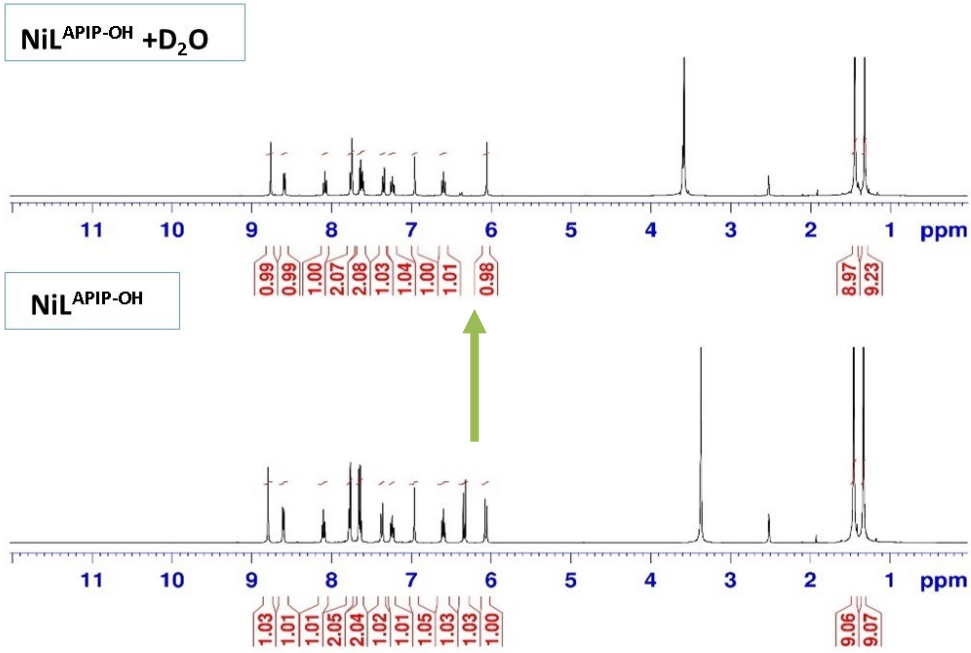

Figure S5. ^1H NMR of $NiL^{APIP-OH}$

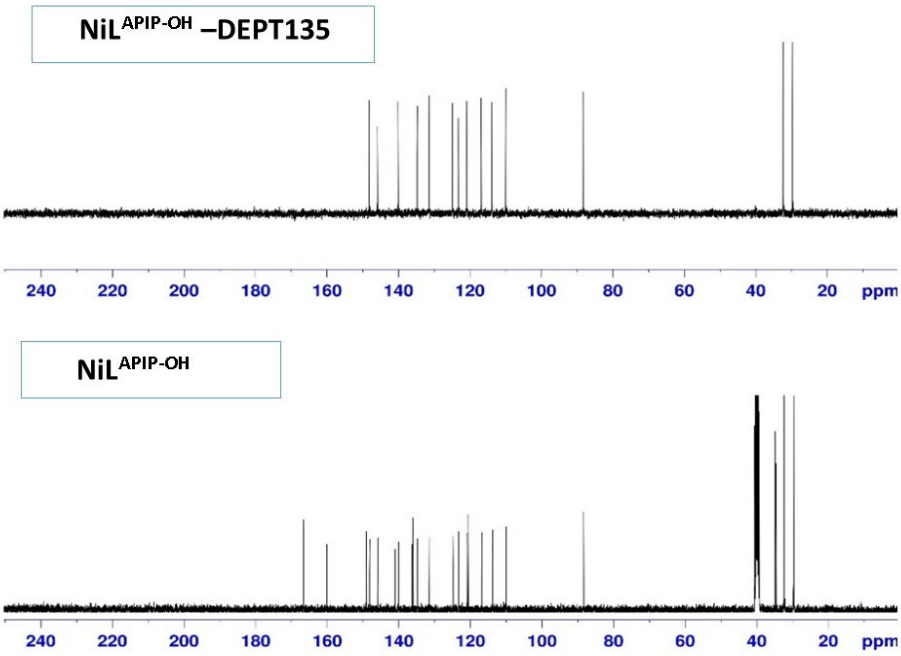

Figure S6. ^{13}C NMR of NiL$^{APIP-OH}$

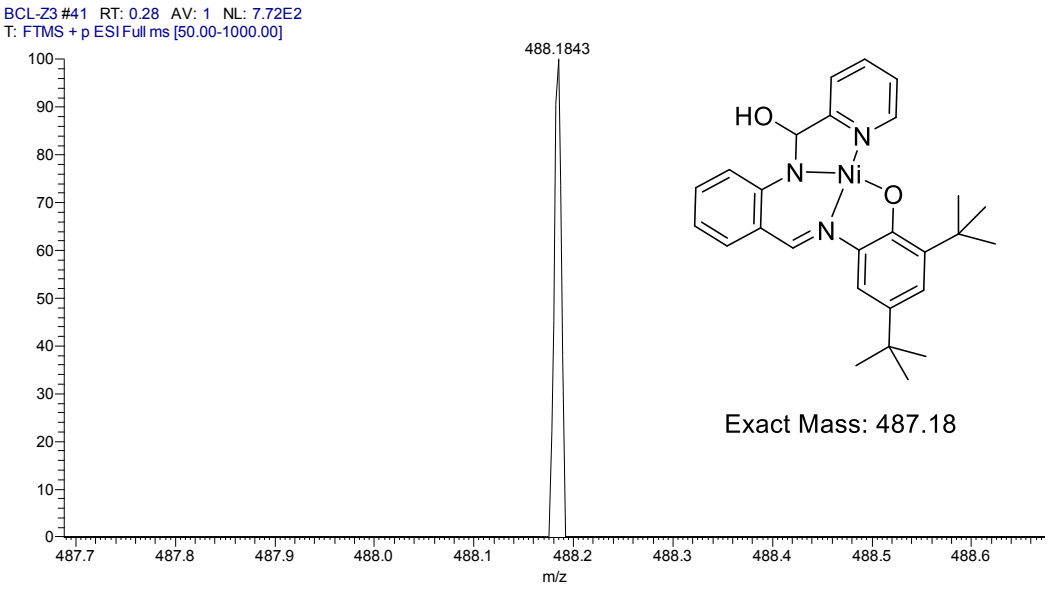

Figure S7. ESI-MS (HRMS) spectrum of NiL$^{APIP-OH}$

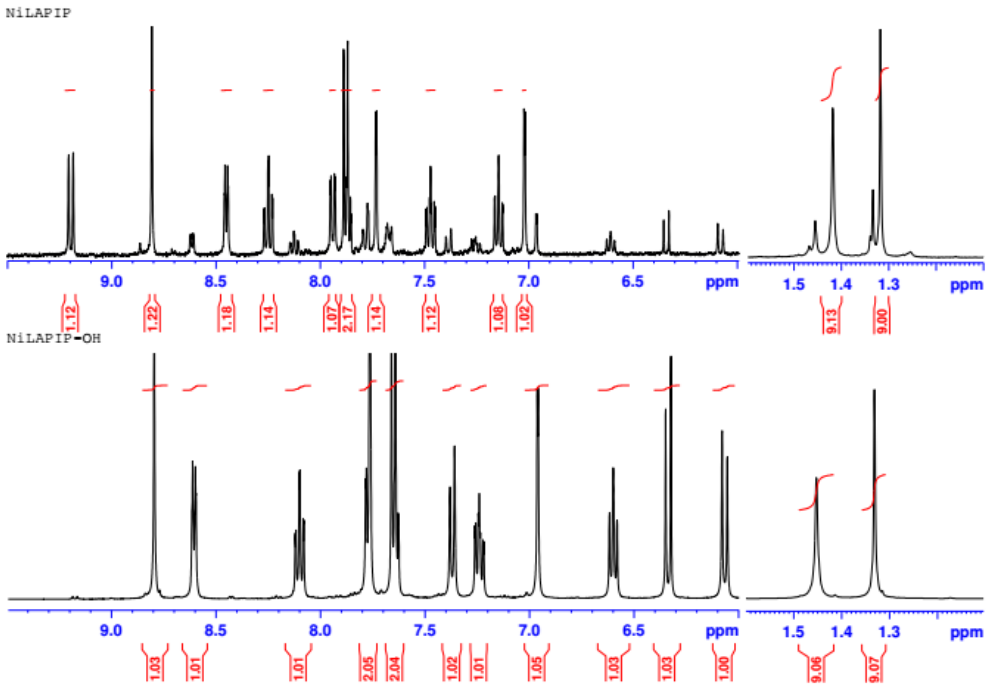

Figure S8. ^{1}H NMR of NiL^{APIP} crystals (top) compare with NiL$^{APIP\text{-}OH}$ (down);
(There is a small amount of NiL$^{APIP\text{-}OH}$ impurity in NiL^{APIP} crystals, revealing gradually oxidation of imine moiety to amide)

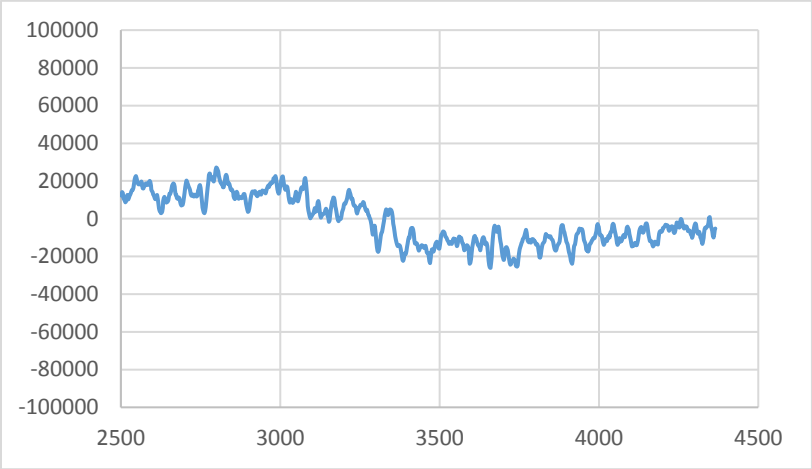

Figure S9. EPR silent spectrum of $Ni^{II}L^{APIP}$

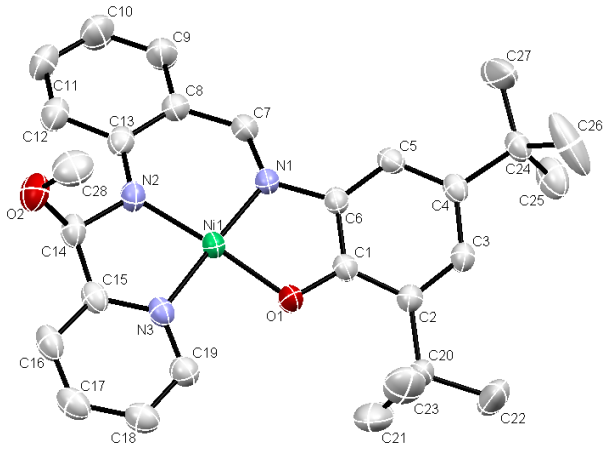

Figure S10. Molecular structure of $Ni^{II}L^{APIP\text{-}OMe}$Hydrogen atoms have been omitted for clarity. Thermal ellipsoids are set at 50 % probability

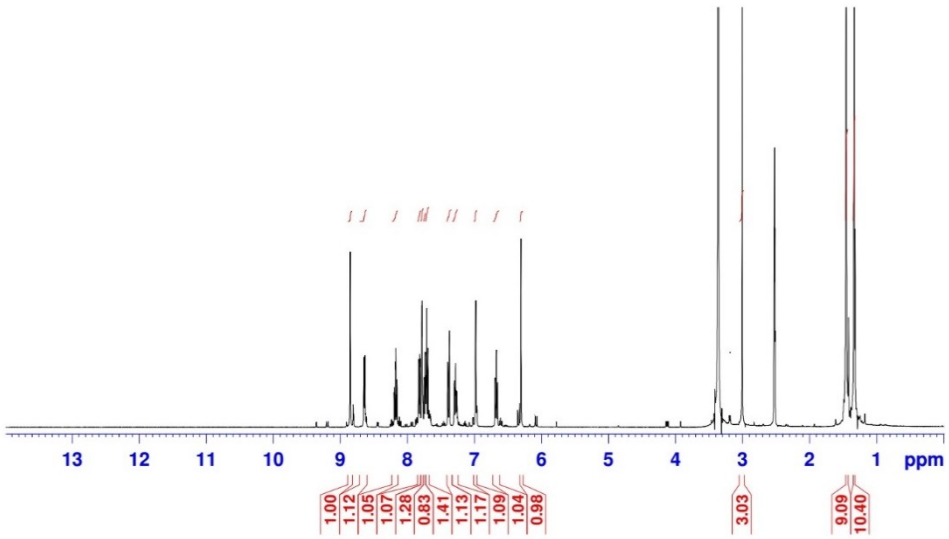

Figure S11. ^{1}H NMR of $Ni^{II}L^{APIP\text{-}MeO}$

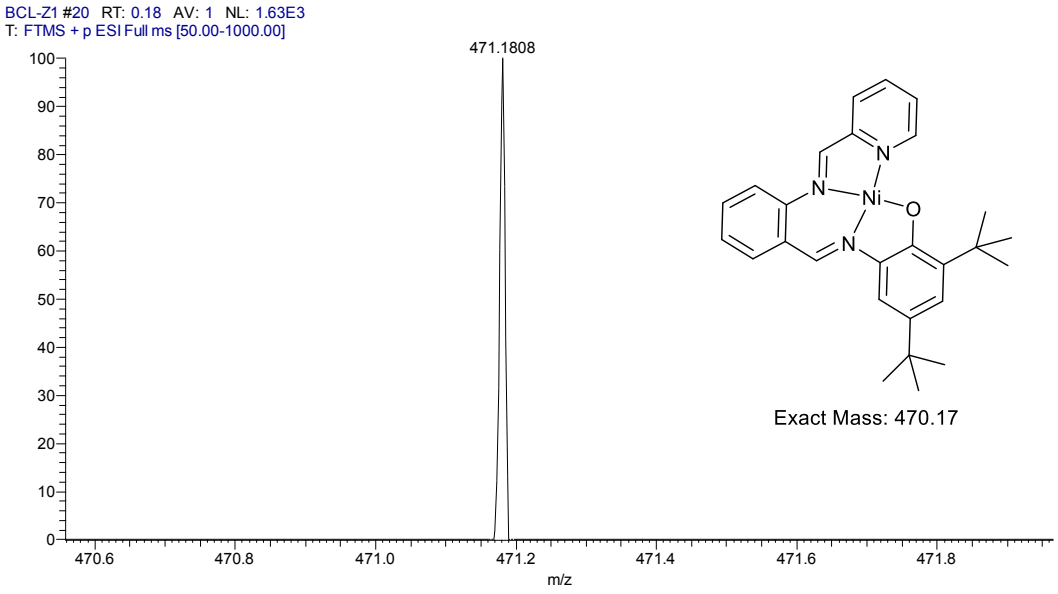

Figure S12. ESI-MS (HRMS) spectrum of NiL^{IPIP}

Table S1. Redox potentials of cyclic voltammogram of $Cu^{II}L^{APIP}$, $Ni^{II}L^{APIP}$ and $Zn^{II}L^{IPIP}OAc$ versus Fc^{+} / Fc^{a}.

compound	$E_{1/2}^{1}$/ V	$E_{1/2}^{2}$/ V
$Cu^{II}L^{APIP}$	+0.41	-1.66
$Ni^{II}L^{APIP}$	+0.51	-1.81
$Zn^{II}L^{IPIP}OAc$	+0.27	-1.47

[a]Peak to peak difference for the Fc^{+} / Fc couple at 298 K is 0.12

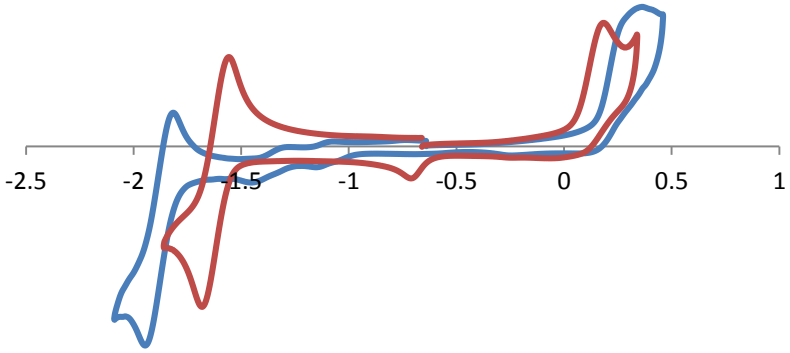

Figure S13. Cyclic voltammogram of $Cu^{II}L^{IPIP}$ (Red), $Ni^{II}L^{IPIP}$ (Blue) Conditions: 2.5 mM complex, 0.1 M $NBu_4(BF_4)$, scan rate 200 mV / s, CH_2Cl_2, 298 K.

Table S2 Redox potentials of cyclic voltammogram of $Cu^{II}L^{IPIP}$ and $Ni^{II}L^{IPIP}$ versus Fc^{+} / Fc^{a}.

compound	$E_{1/2}^{1}$/ V	$E_{1/2}^{2}$/ V
$Cu^{II}L^{IPIP}$	+0.21	-1.60
$Ni^{II}L^{IPIP}$	+0.32	-1.89

X-Ray Crystallography data of Copper, Zinc and nickel complexes

Table S1. Crystallographic data for $Cu^{II}L^{APIP}$

	$Cu^{II}L^{APIP}$
Empirical formula	$C_{27}\ H_{29}\ Cu\ N_3\ O_2$
Formula weight	491.09
Crystal system	Monoclinic
Space group	$P1\ 2_1/c\ 1$
***a* (Å)**	9.5598(5)
***b* (Å)**	18.2903(9)
***c* (Å)**	14.1699(8)
***α* (deg)**	90
***β* (deg)**	107.231(2)
***γ* (deg)**	90
***V* (Å³)**	2366.4(2)
Z	4
***T* (K)**	150(2)
ρ_{calcd} **(g/cm³)**	1.378
***μ* (mm⁻¹)**	0.952
Reflections collected	57791
Significant reflections	9306
***R*[I > 2.5 (*I*)]**	0.0450
R_w**[I > 2.5 (*I*)]**	0.0999
Goodness of fit	0.7317

Table S2. Selected bond lengths of $Cu^{II}L^{APIP}$

Bond	$L^{APIP}Cu^{II}$
Cu(1)-N(2)	1.955 (1.958)
Cu(1)-N(3)	1.955 (1.972)
Cu(1)-N(4)	1.921 (1.924)
Cu(1)-O(5)	1.901 (1.895)
C(17)-O(5)	1.322 (1.326)
C(22)-N(4)	1.414 (1.412)
C(23)-N(4)	1.284 (1.297)
C(6)-N(2)	**1.400 (1.400)**
C(6)-O(2)	**1.230 (1.230)**

Table S3. Crystallographic data for $Cu^{II}L^{IPIP}$

	$L^{IPIP}Cu^{II}$
Empirical formula	C_{29} H_{33} Cu N_4 O
Formula weight	517.14
Crystal system	Orthorhombic
Space group	*Pnma*
a (Å)	24.983(3)
b (Å)	6.9452(7)
c (Å)	16.3797(17)
α (deg)	90.00
β (deg)	90.00
γ (deg)	90.00
V (Å^3)	2842.1
Z	4
T (K)	296
ρ_{calcd} (g/cm^3)	1.209
μ (mm^{-1})	0.794
Significant reflections	6328
R[I > 2.5 (*I*)]	0.0561
R_w[I > 2.5 (*I*)]	0.1637
Goodness of fit	0.997

Table S4. Selected bond lengths of $Cu^{II}L^{IPIP}$

Number	Atom1	Atom2	Length
1	Cu1	N1	1.965
2	Cu1	O1	1.912
3	Cu1	N2	1.903
4	Cu1	N3	1.928
5	H1	C1	1.01
6	N1	C1	1.343
7	N1	C5	1.322
8	O1	C19	1.331
9	C1	C2	1.372
10	C2	H2	0.82
11	C2	C3	1.37
12	N2	C7	1.366
13	N2	C6	1.44
14	C3	H3	0.85
15	C3	C4	1.385
16	N3	C13	1.298
17	N3	C14	1.417
18	C4	H4	0.995

Table S5. Crystallographic data for $Cu^{II}L^{APIP\text{-}MeO}$

	$Cu^{II}L^{APIP\text{-}MeO}$
Empirical formula	$C_{28}\ H_{33}\ Cu\ N_3\ O_2$
Formula weight	507.12
Crystal system	Orthorhombic
Space group	*Pbca*
a (Å)	15.8660(8)
b (Å)	14.5267(7)
c (Å)	22.0264(11)
α (deg)	90.00
β (deg)	90.00
γ (deg)	90.00
V (Å^3)	5076.66
Z	8
T (K)	296
ρ_{calcd} (g/cm^3)	1.327
μ (mm^{-1})	0.890
Significant reflections	6328
R[I > 2.5□ (*I*)]	0.0470
R_w[I > 2.5□ (*I*)]	0.1261
Goodness of fit	0.997

Table S6. Selected bond lengths of $Cu^{II}L^{APIP\text{-}MeO}$

Number	Atom1	Atom2	Length
1	Cu1	N1	1.963(2)
2	Cu1	N2	1.911(2)
3	Cu1	N3	1.919(2)
4	Cu1	O1	1.902(2)
5	N1	C5	1.333(3)
6	N1	C1	1.339(4)
7	N2	C6	1.429(4)
8	N2	C7	1.368(3)
9	N3	C14	1.423(3)
10	N3	C13	1.293(3)
11	O1	C19	1.320(3)
12	C4	C5	1.379(4)
13	C4	C3	1.367(5)
14	C4	H4	0.88(3)
15	C5	C6	1.508(4)
16	C6	H6	1.09(2)
17	C6	O2	1.451(3)
18	C1	C2	1.368(4)
19	C1	H1	0.91(3)
20	C2	C3	1.366(5)

21	C2	H2	0.85(3)
22	C3	H3	0.86(3)
23	C19	C14	1.407(4)
24	C19	C18	1.418(4)
25	C14	C15	1.391(4)
26	C18	C17	1.382(4)
27	C18	C20	1.538(4)
28	C16	C15	1.378(4)
29	C16	C17	1.396(4)
30	C16	C24	1.537(4)
31	C13	C12	1.433(4)
32	C13	H13	0.92(3)
33	C15	H15	0.89(2)
34	C12	C7	1.426(4)
35	C12	C11	1.409(4)
36	C7	C8	1.419(4)
37	C11	C10	1.362(5)
38	C11	H11	0.89(3)
39	C17	H17	0.93(3)

Table S7. Crystallographic data for $ZnL^{APIP}OAc$

	$Zn^{II}L^{APIP}OAc$
Empirical formula	C29 H34 N3 O3.50 Zn
Formula weight	545.96
Temperature, K	293(2)
Wavelength; Å	0.71073
Crystal system, space group	Triclinic, P-1
Unit cell dimensions; Å,°	a = 10.1927(13)
	b = 10.2059(12)
	c = 14.7907(19)
	alpha = 94.834(10)
	beta = 98.779(11)
	gamma = 114.583(12)
Volume; $Å^3$	1364.0(3)
Z, Calculated density; Mg/m^3	2, 1.329
Absorption coefficient; mm^{-1}	0.937
Goodness-of-fit on F^2	1.073
Final R indices [I>2sigma(I)]	R1 = 0.0631, wR2 = 0.1711
R indices (all data)	R1 = 0.0871, wR2 = 0.2184
Largest diff. peak and hole; $e.Å^{-3}$	0.891 and -0.568

Table S8. Bond lengths of $ZnL^{IPIP}OAc$

Bond length			Angles	
Zn1-O1	1.978(3)		O1-Zn1-O2	**111.95(14)**
Zn1-O2	1.991(4)		O1-Zn1-N1	**81.73(12)**
Zn1-N1	2.087(3)		O2-Zn1-N1	**117.06(15)**
Zn1-N3	2.109(4)		O1-Zn1-N3	**96.71(13)**
Zn1-N2	2.174(3)		O2-Zn1-N3	**105.45(15)**
O1-C1	1.311(5)		N1-Zn1-N3	**134.79(14)**
C1-C2	1.431(5)		O1-Zn1-N2	**153.35(14)**
C1-C6	1.432(5)		O2-Zn1-N2	**94.67(13)**
C2-C3	1.392(5)		N1-Zn1-N2	**85.04(13)**
C2-C20	1.543(5)		N3-Zn1-N2	**76.60(13)**
C3-C4	1.391(6)		C1-O1-Zn1	**114.7(2)**
C4-C5	1.390(6)		O1-C1-C2	**123.0(3)**
C4-C24	1.546(6)		O1-C1-C6	**119.8(3)**
C5-C6	1.386(5)		C2-C1-C6	**117.1(3)**
C6-N1	1.426(5)		C3-C2-C1	**119.1(3)**
N1-C7	1.281(5)		C3-C2-C20	**121.3(4)**
C7-C8	1.471(6)		C1-C2-C20	**119.6(3)**
C8-C9	1.394(6)		C4-C3-C2	**123.5(4)**
C8-C13	1.428(6)		C5-C4-C3	**117.5(4)**
C9-C10	1.390(6)		C5-C4-C24	**121.5(4)**
C10-C11	1.364(7)		C3-C4-C24	**121.1(4)**
C11-C12	1.383(7)		C6-C5-C4	**121.8(4)**
C12-C13	1.394(6)		C5-C6-N1	**125.2(4)**
C13-N2	1.419(5)		C5-C6-C1	**121.1(4)**
N2-C14	1.249(6)		N1-C6-C1	**113.6(3)**
C14-C15	1.465(6)		C7-N1-C6	**123.5(3)**
C15-N3	1.354(6)		C7-N1-Zn1	**126.2(3)**
C15-C16	1.374(6)		C6-N1-Zn1	**110.1(2)**
C16-C17	1.389(7)		N1-C7-C8	**127.2(4)**
C17-C18	1.400(8)		C9-C8-C13	**116.8(4)**
C18-C19	1.380(7)		C9-C8-C7	**116.5(4)**
C19-N3	1.326(6)		C13-C8-C7	**126.7(4)**
C20-C21	1.528(7)		C10-C9-C8	**121.7(4)**
C20-C23	1.531(7)		C11-C10-C9	**120.9(4)**
C20-C22	1.552(6)		C10-C11-C12	**119.7(4)**
C24-C27	1.493(9)		C11-C12-C13	**120.6(4)**
C24-C25	1.502(7)		C12-C13-N2	**121.8(4)**
C24-C26	1.569(8)		C12-C13-C8	**120.4(4)**
O2-C28	1.209(7)		N2-C13-C8	**117.8(4)**
C28-O3	1.246(7)		C14-N2-C13	**121.6(4)**
C28-C29	1.528(9)		C14-N2-Zn1	**114.3(3)**
			C13-N2-Zn1	**124.0(3)**
			N2-C14-C15	**118.9(4)**
			N3-C15-C16	**122.5(4)**
			N3-C15-C14	**115.5(4)**
			C16-C15-C14	**121.9(4)**
			C15-C16-C17	**118.6(5)**
			C16-C17-C18	**118.7(5)**
			C19-C18-C17	**119.1(5)**
			N3-C19-C18	**122.0(5)**

Table S9. Crystallographic data for $Ni^{II}L^{APIP}$

	$Ni^{II}L^{APIP}$
Empirical formula	$C_{27}\ H_{29}\ Ni\ N_3\ O_2$
Formula weight	486.22
Crystal system	Monoclinic
Space group	$P\ 2_1/c$
***a* (Å)**	9.7052(6)
***b* (Å)**	18.0704(11)
***c* (Å)**	14.1301(10)
***α* (deg)**	90
***β* (deg)**	107.8527(15)
***γ* (deg)**	90
***V* (Å³)**	2358.77
Z	4
***T* (K)**	296
ρ_{calcd} **(g/cm³)**	1.369
***μ* (mm⁻¹)**	0.852
***R*[I > 2.5□ (*I*)]**	0.04361
R_w**[I > 2.5□ (*I*)]**	0.1353
Goodness of fit	0.7317

Table S10. Selected bond lengths of $Ni^{II}L^{APIP}$

Atom1	Atom2	Length
Ni1	N1	1.846(2)
Ni1	O1	1.838(2)
Ni1	N2	1.885(2)
Ni1	N3	1.888(2)
N1	C13	1.287(4)
N1	C14	1.417(3)
O1	C19	1.333(2)
C1	C2	1.378(4)
C1	N2	1.329(4)
C2	H2	0.929(3)
C2	C3	1.378(4)
O2	C6	1.224(3)
N2	C5	1.342(3)
C3	H3	0.929(3)
C3	C4	1.379(4)
N3	C6	1.379(3)
N3	C7	1.393(4)
C5	C6	1.487(4)
C5	C4	1.380(4)
C7	C8	1.410(4)
C7	C12	1.412(4)

Table S11. Crystallographic data for for monoclinic form of $Ni^{II}L^{APIP\text{-}MeO}$

	$Ni^{II}L^{APIP\text{-}MeO}$
Empirical formula	C28 H33 N3 Ni O2
Formula weight	502.28
Crystal system	Monoclinic
Space group	$P\ 2_1/c$
***a* (Å)**	11.5267(8) A
***b* (Å)**	16.6156(10) A
***c* (Å)**	13.6845(9)
***α* (deg)**	90
***β* (deg)**	104.524(7)
***γ* (deg)**	90
***V* (Å³)**	2537.1(3)
Z	4
***T* (K)**	298
ρ_{calcd} **(g/cm³)**	1.315
***R*[I > 2.5 (*I*)]**	R1 = 0.0339
R_w**[I > 2.5 (*I*)]**	wR2 = 0.0869
Goodness of fit	1.073

Table S12. Selected bond lengths for monoclinic form of $Ni^{II}L^{APIP\text{-}MeO}$

Number	Atom1	Atom2	Length
1	Ni1	O1	1.843(2)
2	Ni1	N1	1.844(2)
3	Ni1	N2	1.852(2)
4	Ni1	N3	1.882(2)
5	**O1**	**C1**	**1.331(4)**
6	C1	C2	1.413(4)
7	C1	C6	1.408(4)
8	C2	C3	1.385(4)
9	C2	C20	1.537(5)
10	C3	H3A	0.93
11	C3	C4	1.409(4)
12	C4	C5	1.386(4)
13	C4	C24	1.538(4)
14	C5	H5A	0.93
15	C5	C6	1.396(4)
16	**C6**	**N1**	**1.425(3)**
17	N1	C7	1.308(4)
19	C7	C8	1.420(4)
20	C8	C9	1.417(4)
21	C8	C13	1.431(4)
23	C9	C10	1.360(4)
25	C10	C11	1.400(5)
27	C11	C12	1.376(5)
29	C12	C13	1.418(4)
30	C13	N2	1.367(4)
31	**N2**	**C14**	**1.448(4)**
33	C14	C15	1.504(4)
34	**C14**	**O2**	**1.438(3)**

Table S13. Crystallographic data for triclinic form of $Ni^{II}L^{APIP\text{-}MeO}$

Identification code	**$Ni^{II}L^{APIP\text{-}MeO}$ e712a**
Empirical formula	C28 H33 N3 Ni O2
Formula weight	502.28
Temperature	293(2) K
Wavelength	0.71073 Å
Crystal system	Triclinic
Space group	P-1
Unit cell dimensions	a = 9.3643(8) Å
	b = 9.9780(8) Å
	c = 14.3688(12) Å
	α = 101.276(7)°.
	β = 95.203(7)°.
	γ = 99.728(7)°.
Volume	1287.04(19) $Å^3$
Z	2
Density (calculated)	1.296 Mg/m^3
Absorption coefficient	0.783 mm^{-1}
F(000)	532
Crystal size	0.544 x 0.318 x 0.130 mm^3
Theta range for data collection	2.225 to 28.096°.
Index ranges	-6<=h<=12, -12<=k<=11, -17<=l<=18
Reflections collected	8310
Independent reflections	5514 [R(int) = 0.0542]
Completeness to theta = 25.000°	99.9 %
Absorption correction	Analytical
Max. and min. transmission	0.909 and 0.725
Refinement method	Full-matrix least-squares on F^2
Data / restraints / parameters	5514 / 0 / 307
Goodness-of-fit on F^2	1.028
Final R indices [I>2sigma(I)]	R1 = 0.0470, wR2 = 0.1246
R indices (all data)	R1 = 0.0671, wR2 = 0.1377
Extinction coefficient	n/a
Largest diff. peak and hole	0.408 and -0.517 $e.Å^{-3}$

Table S14. Selected bond lengths for triclinic form of $Ni^{II}L^{APIP\text{-}MeO}$

Bond		Angle	
Ni1-O1	1.8431(18)	O1-Ni1-N1	**86.58(8)**
Ni1-N1	1.844(2)	O1-Ni1-N2	**175.97(9)**
Ni1-N2	1.853(2)	N1-Ni1-N2	**96.36(9)**
Ni1-N3	1.881(2)	O1-Ni1-N3	**91.35(9)**
O1-C1	1.330(3)	N1-Ni1-N3	**177.69(9)**
C1-C6	1.408(3)	N2-Ni1-N3	**85.77(9)**
C1-C2	1.413(3)	C1-O1-Ni1	**113.08(16)**
C2-C3	1.386(4)	O1-C1-C6	**116.8(2)**
C2-C20	1.537(4)	O1-C1-C2	**124.2(2)**
C3-C4	1.409(4)	C6-C1-C2	**119.0(2)**
C4-C5	1.385(3)	C3-C2-C1	**116.9(2)**
C4-C24	1.539(3)	C3-C2-C20	**122.7(2)**
C5-C6	1.395(3)	C1-C2-C20	**120.4(2)**
C6-N1	1.425(3)	C2-C3-C4	**124.7(2)**
N1-C7	1.308(3)	C5-C4-C3	**117.4(2)**
C7-C8	1.422(3)	C5-C4-C24	**123.3(2)**
C8-C9	1.418(4)	C3-C4-C24	**119.3(2)**
C8-C13	1.429(4)	C4-C5-C6	**119.7(2)**
C9-C10	1.360(4)	C5-C6-C1	**122.1(2)**
C10-C11	1.401(4)	C5-C6-N1	**126.7(2)**
C10-H10A	0.9300	C1-C6-N1	**111.2(2)**
C11-C12	1.376(4)	C7-N1-C6	**121.9(2)**
C12-C13	1.418(3)	C7-N1-Ni1	**125.88(18)**
C13-N2	1.367(3)	C6-N1-Ni1	**112.19(16)**
N2-C14	1.448(3)	N1-C7-C8	**125.5(2)**
C14-O2	1.437(3)	C9-C8-C7	**116.5(2)**
C14-C15	1.505(4)	C9-C8-C13	**119.5(2)**
C15-N3	1.346(3)	C7-C8-C13	**123.9(2)**
C15-C16	1.381(4)	C10-C9-C8	**122.6(3)**
C16-C17	1.378(5)	C9-C10-C11	**117.9(3)**
C17-C18	1.389(5)	C12-C11-C10	**121.7(3)**
C18-C19	1.366(4)	C11-C12-C13	**121.7(3)**
C19-N3	1.349(4)	N2-C13-C12	**122.8(2)**
C20-C23	1.520(5)	N2-C13-C8	**120.7(2)**
C20-C21	1.530(4)	C12-C13-C8	**116.5(2)**
C20-C22	1.534(5)	C13-N2-C14	**117.0(2)**
C24-C27	1.521(4)	C13-N2-Ni1	**127.27(18)**
C24-C26	1.524(4)	C14-N2-Ni1	**115.36(18)**
C24-C25	1.529(4)	O2-C14-N2	**115.0(2)**
O2-C28	1.405(4)	O2-C14-C15	**109.2(2)**
		N2-C14-C15	**108.8(2)**
		N3-C15-C16	**121.9(3)**
		N3-C15-C14	**114.9(2)**
		C16-C15-C14	**123.1(3)**
		C17-C16-C15	**119.4(3)**
		C16-C17-C18	**118.7(3)**
		C19-C18-C17	**119.1(3)**
		N3-C19-C18	**122.6(3)**
		C15-N3-C19	**118.3(3)**
		C15-N3-Ni1	**114.97(19)**
		C19-N3-Ni1	**126.8(2)**
		C23-C20-C21	**107.9(3)**
		C23-C20-C22	**109.4(3)**
		C21-C20-C22	**108.4(3)**